Islamic University Journal of Applied Sciences (IUJAS)

https://journals.iu.edu.sa/jesc

Volume VIII, Issue I, July 2026, Pages 168-188

Theoretical investigation using DFT Calculations, Vibrational Assignments, Infrared Spectrum and Normal Coordinate Analysis of (2-Chloro-4-fluorophenyl) boronic Acid

Usama A. Soliman[1]*

[1] Chemistry Division, Department of Physical Sciences, College of Science, Jazan University, P.O. Box. 114, Jazan, 45142, Kingdom of Saudi Arabia.

* Corresponding author: (Usama A. Soliman) , *Email Address*: usoliman@jazanu.edu.sa

Abstract

The geometry, vibrational frequencies, and thermodynamic parameters of 2-chloro-4-fluorophenylboronic acid (CFPB; $C_6H_5BClFO_2$) have been computed using the Gaussian 09 software package. Initially, four distinct rotamers were proposed for this compound, arising from the internal rotation of the hydroxyl groups around the C–B bond. A conformational stability analysis for an isolated molecule was performed using the B3LYP functional with the standard 6-311++G(d,p) basis set. Our calculations identified the CT structure where one OH group is *cis* to both the phenyl Cl and F atoms, and the other OH is *trans* to the phenyl Cl atom—as the most stable conformation. The energy differences between the CT conformer and the others (2-4) range from 1700 to 2000 cm^{-1} (4.88 – 5.72 kcal/mol). This stability is attributed to stabilizing O_5...H14 and Cl_6....H15 intramolecular hydrogen bonds. A complete vibrational assignment of the observed IR bands is provided, supported by calculated wavenumbers, IR intensities, and a normal coordinate analysis. The computed wavenumbers and IR intensities for the CT form agree well with the experimental data.

Keywords: 2-Chloro-4-fluorophenylboronic acid; B3LYP calculations; Infrared spectroscopy; Normal coordinate analysis.

https://doi.org/10.63070/jesc.2026.022

Received 17 January 2026; Revised 27 March 2026; Accepted 10 April 2026.

Available online 15 April 2026.

Published by Islamic University of Madinah on behalf of *Islamic University Journal of Applied Sciences*.

This is an open access article published under the Creative Commons Attribution 4.0 International license (CC BY 4.0):https://creativecommons.org/licenses/by/4.0/

1. Introduction

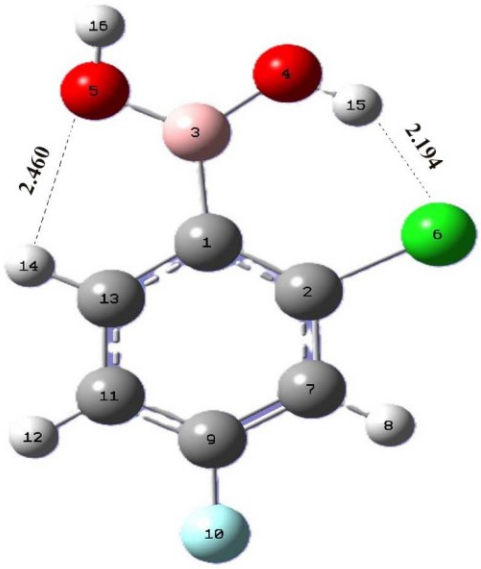
Boronic acid derivatives represent a class of compounds of significant interest due to their broad applications in pharmaceuticals [1,2] and diverse physiological activities [3,4]. They are also vital in synthesizing chemical building blocks, intermediates [5], biaryl compounds [6,7], and antihypertensive agents [8]. Their biological utility extends to roles as enzyme inhibitors, catalysts, protecting groups, saccharide-sensing receptors, neutron capture therapy agents, and anti-metabolites for cancer treatment [9-12]. Phenylboronic acid, featuring a phenyl ring substituted with a boron atom bonded to two hydroxyl groups, is a fundamental structure among these derivatives. The single-crystal X-ray structure of phenylboronic acid was determined by Rettig and Trotter [16], while its dimer was reported by Cyrański et al. [17]. The structure of 2,4-difluorophenylboronic acid was detailed by Rodriguez et al. [18]. Additionally, X-ray diffraction studies have been conducted on 4-chloro- and 4-bromophenylboronic acids, as well as the hydrates of 2- and 4-iodophenylboronic acid [19]. The infrared spectra of phenylboronic acid [20], diphenyl phenylboronate [20], and several derivatives—including 4-chloro- [21], 3-bromo- [22], 3,5-dichloro- [23,24], and 2,6-dimethoxyphenylboronic acid [25] have been examined both experimentally and theoretically. Conformational analysis, vibrational spectra, and electronic transitions have also been explored for 2,3- and 3,5-difluorophenylboronic acid molecules [26,27] and methylboronic acid [28]. To the best of our knowledge, a comprehensive theoretical or experimental study on 2-chloro-4-fluorophenylboronic acid (CFPB) has not been reported, although its IR spectrum is not available. This study aims to address this gap by investigating the conformational stability and vibrational assignments of CFPB using DFT quantum mechanical calculations. We also performed a normal coordinate analysis to elucidate the normal modes of vibration, supported by potential energy distributions (PEDs) and force constant determinations.

2. Computational Details

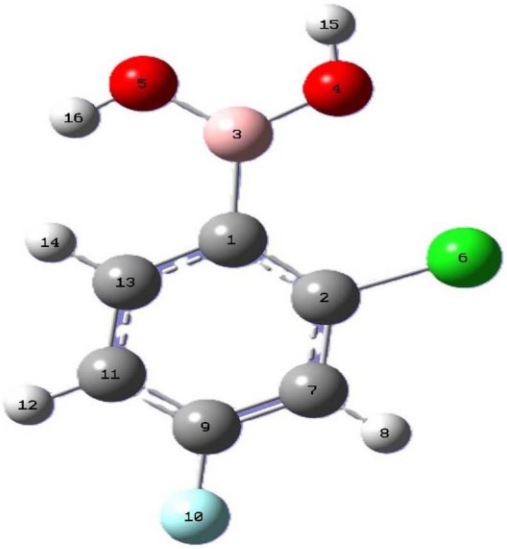
2.1. Conformational Isomerism and DFT Calculations

The rotational isomerism in CFPB (with an assumed C_s symmetry) arises from the two hydroxyl groups attached to the boron atom, which is connected to the phenyl ring at the C_1 position. These structures are designated as **CT, TC, TT, and CC**, where 'C' denotes *cis* and 'T' denotes *trans* orientations of the OH groups relative to the phenyl C_1 atom. Calculating vibrational spectra is computationally more intensive than geometry optimization [29], as it requires a normal mode analysis involving the second derivatives of energy with respect to nuclear displacements.

For molecules of moderate size, Density Functional Theory (DFT) calculations have proven highly effective for both structural and frequency analyses [30, 31]. The availability of analytical second derivative techniques has significantly advanced quantum mechanical calculations, making vibrational frequency computations feasible for larger molecules [32]. Optimizing the CFPB conformers can be sensitive to initial approximations, and shifts in nuclear positions during optimization may lead to saddle points or local energy minima. Saddle points are problematic as they yield imaginary vibrational frequencies, while local minima can misrepresent conformational interconversions and vibrational spectral features. The inherent flexibility and mobility of the hydroxyl group around the single bond, coupled with potential intramolecular hydrogen bonding, contribute to these optimization challenges. To mitigate these issues, the molecular geometry of 2-chloro-4-fluorophenylboronic acid was constrained to C_s symmetry during the optimization and frequency calculations for all conformers. Geometry optimizations for the CFPB conformers **(Fig. 1)** were performed using the hybrid B3LYP functional [33-35] and the 6-311++G(d,p) basis set, as implemented in the Gaussian 09 package [36]. This basis set includes polarization and diffusion functions. Energy minima with respect to nuclear coordinates were located by relaxing all geometric parameters simultaneously using the Pulay gradient method [37], with specific dihedral angles constrained to maintain C_s symmetry. Vibrational frequencies were subsequently calculated at the same level of theory. Full convergence was achieved, with the maximum force below 0.00045 mdyne and the maximum displacement below 0.0018 Å. The B3LYP/6-311++G(d,p) results conclusively identified the CT structure **(Conformer 1 in Fig. 1)** as the global minimum, characterized by the lowest energy. In contrast, the other isomers (TC, TT, CC) were identified as transition states, as evidenced by their higher relative energies and the presence of one imaginary frequency in their vibrational analysis; they were therefore excluded from further analysis. The energy differences between the CT conformer and the others (2-4) range from 1700 to 2000 cm^{-1} (4.88 – 5.72 kcal/mol), as illustrated in **Fig. 1**. Selected structural parameters (SPs) calculated at the B3LYP/6-31G(d) and B3LYP/6-311++G(d,p) levels for the most stable CT conformer are listed in **Table 1**, alongside X-ray crystallographic data for relevant phenylboronic acid derivatives [16,38,18].

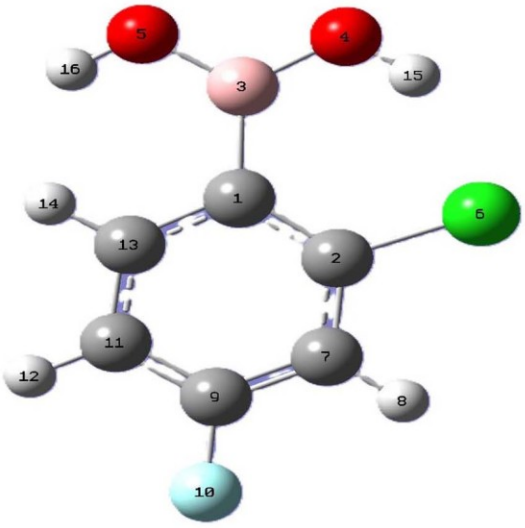


Structure CT
Minimum



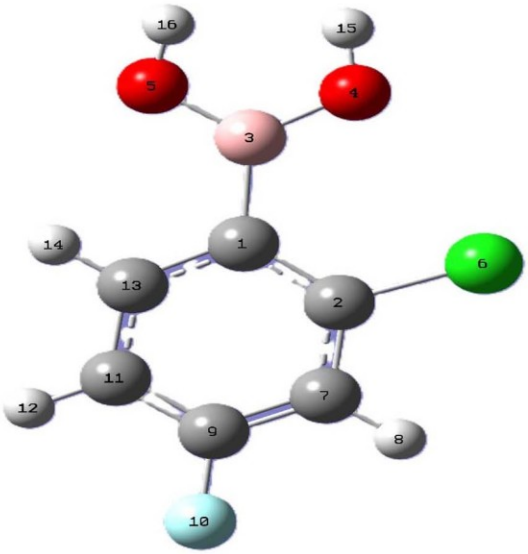
Structure TC

ΔE= 1720cm^{-1}(4.92 kcal/mol)
1707cm^{-1}(4.88 kcal/mol)



Structure CC

ΔE= 1728cm^{-1}(4.94 kcal/mol)
1722cm^{-1}(4.92 kcal/mol)



Structure TT

ΔE= 2000cm^{-1}(5.72 kcal/mol)
1930cm^{-1}(5.52 kcal/mol)

Fig 1. Total energies differences (***bold italic*** utilizing 6-311++G** and normal line utilizing 6-31G* basis sets) between **CT** conformer and other **CC, TT** and **TC** conformers at b3lyp method in cm^{-1}and kcal/mol

TABLE.1. B3LYP structural parameters for 2-Chloro-4-florophenylboronic acid (conformer CT) utilizing 6-31G(d) and 6-311++G(d,p) basis sets.

Parameters	X-ray Ref. [16]	X-ray Ref. [38]	X-ray Ref. [18]	*B3LYP for Structure(CT)* 6-31G(d)	6-311++G(d,p)
r($C_1C_{2\ ring}$)	1.404	1.406	1.382	1.405	1.402
r($C_2C_{7\ ring}$)	1.389	1.377	1.370	1.394	1.391
r($C_7C_{9\ ring}$)	1.378	1.365	1.363	1.389	1.385
r ($C_9C_{11\ ring}$)	1.384	1.375	1.366	1.389	1.385
r($C_{11}C_{13\ ring}$)	1.390	1.387	1.374	1.391	1.389
r($C_{13}C_{1ring}$)	1.402	1.398	1.394	1.414	1.412
r($C_7H_{8\ ring}$)	1.00	0.93	0.93	1.083	1.081
r($C_{11}H_{12\ ring}$)	1.00	0.93	0.93	1.085	1.082
r($C_{13}H_{14\ ring}$)	1.00	0.93	0.93	1.086	1.083
r(C_2— Cl_6)	—	—	—	1.780	1.777
r(C_9—F_{10})	—	—	1.364	1.345	1.350
r(C_1—B_3)	1.568	1.562	1.566	1.583	1.579
r(B_3—O_4)	1.378	1.343	1.388	1.367	1.366
r(B_3—O_5)	1.362	1.366	1.361	1.367	1.366
r(O_4H_{15})	0.75	0.855	0.841	0.968	0.963
r(O_5H_{16})	0.75	0.855	0.841	0.968	0.963
r(Cl.....H_{15})	—	—	2.16	2.200	2.194
r(O_5.....H_{14})	—	—	—	2.453	2.460
∠($C_1C_2C_7$)	121.8	123.9	125.1	123.4	123.2
∠($C_2C_7C_9$)	119.5	118.6	116.4	118.2	118.1
∠($C_7C_9C_{11}$)	120.3	118.4	123.0	121.9	122.2
∠($C_9C_{11}C_{13}$)	120.1	119.7	117.9	117.8	117.7
∠($C_{11}C_{13}C_1$)	121.1	121.8	122.9	123.6	123.5
∠($C_{13}C_1C_2$)	117.2	117.6	114.6	115.0	115.3
∠($C_2C_1B_3$)	122.0	122.1	125.3	129.3	128.9
∠ ($C_{13}C_1B_3$)	120.8	120.1	120.1	115.6	115.8
∠ ($C_1B_3O_4$)	118.7	119.0	123.8	121.3	121.3
∠ ($C_1B_3O_5$)	125.0	122.7	117.4	121.3	121.3
∠ ($B_3O_4H_{15}$)	111.0	116.0	116.0	111.8	113.2
∠ ($B_3O_5H_{16}$)	111.0	124.0	115.0	111.8	113.2
∠ ($O_4B_3O_5$)	116.3	118.2	118.7	117.5	117.4
∠ ($C_1C_2Cl_6$)	120.0	—	—	122.2	122.2
∠ ($C_7C_2Cl_6$)	120.0	—	—	114.5	114.6
∠ ($C_2C_7H_8$)	120.0	—	121.8	121.6	121.6
∠ ($C_9C_7H_8$)	120.0	—	121.8	120.2	120.3
∠ ($C_7C_9F_{10}$)	—	118.1	118.2	118.5	118.4
∠ ($C_{11}C_9F_{10}$)	—	118.0	116.7	119.6	119.4
∠ ($C_9C_{11}H_{12}$)	120.0	119.1	121.0	120.0	120.2
∠ ($C_{13}C_{11}H_{12}$)	120.0	119.1	121.0	122.1	122.1
∠ ($C_{11}C_{13}H_{14}$)	120.0	120.7	118.5	118.9	119.0
∠ ($C_1C_{13}H_{14}$)	120.0	120.7	118.5	117.4	117.6

2.2. Calculated IR Spectra

The IR spectrum of the CT conformer was simulated using the computed wavenumbers and IR intensities and compared with the experimentally observed spectra recorded in KBr disk and Nujol mull **(Figs. 2A, 2B)** from Ref. [39]. The frequencies and infrared intensities were derived from the *ab initio* calculations. IR intensities were determined based on the derivatives of the dipole moment with respect to Cartesian coordinates. These derivatives, obtained from the *ab initio* output, were transformed into normal coordinates using the equation[39]: using $\frac{\partial \mu_u}{\partial Q_i} = \left(\sum_j \frac{\partial \mu_u}{\partial X_j}\right) L_{ij}$,where$Q_i$ is the ith Cartesian displacement coordinate, and $L_{ij}$is the transformation matrix between the Cartesian displacement coordinates and normal coordinates. The infrared intensities were then calculated with the following formula[39]: $I_i = \frac{N\pi}{3c^2}\left[\left(\frac{\partial \mu_x}{\partial Q_i}\right)^2 + \left(\frac{\partial \mu_y}{\partial Q_i}\right)^2 + \left(\frac{\partial \mu_z}{\partial Q_i}\right)^2\right]$. The simulated IR spectrum is in reasonably good agreements with the observed spectrum of the sample with the exception of some bands with high intensities are reversed in the calculated spectrum.

2.3. Normal Coordinate Analysis

The molecule possesses 42 fundamental vibrational modes, distributed as 29 in-plane (A') and 13 out-of-plane (A") modes, all of which are both IR and Raman active. A set of 55 internal coordinates **(Fig. 3)** was used to construct 42 local symmetry coordinates **(Table 2)** following Wilson's GF matrix method [40]. While 13 of these internal coordinates are redundant, they are necessary for determining the force constants. The Cartesian coordinates from the optimized structure were input into a G-matrix program to generate the B-matrix, which was then used in an F-matrix program similar to the one developed by Schachtschneider [41]. This program converts the force constants (FCs) from Cartesian coordinates into FCs in the chosen internal coordinates. The resulting diagonal FCs in internal coordinates, along with the implemented scaling factors (SFs), are listed in **Table 3**. These FCs were employed in a mass-weighted Cartesian coordinate calculation to reproduce the vibrational frequencies and determine the potential energy distributions (PEDs). It is well-known that theoretical FCs and vibrational frequencies tend to be

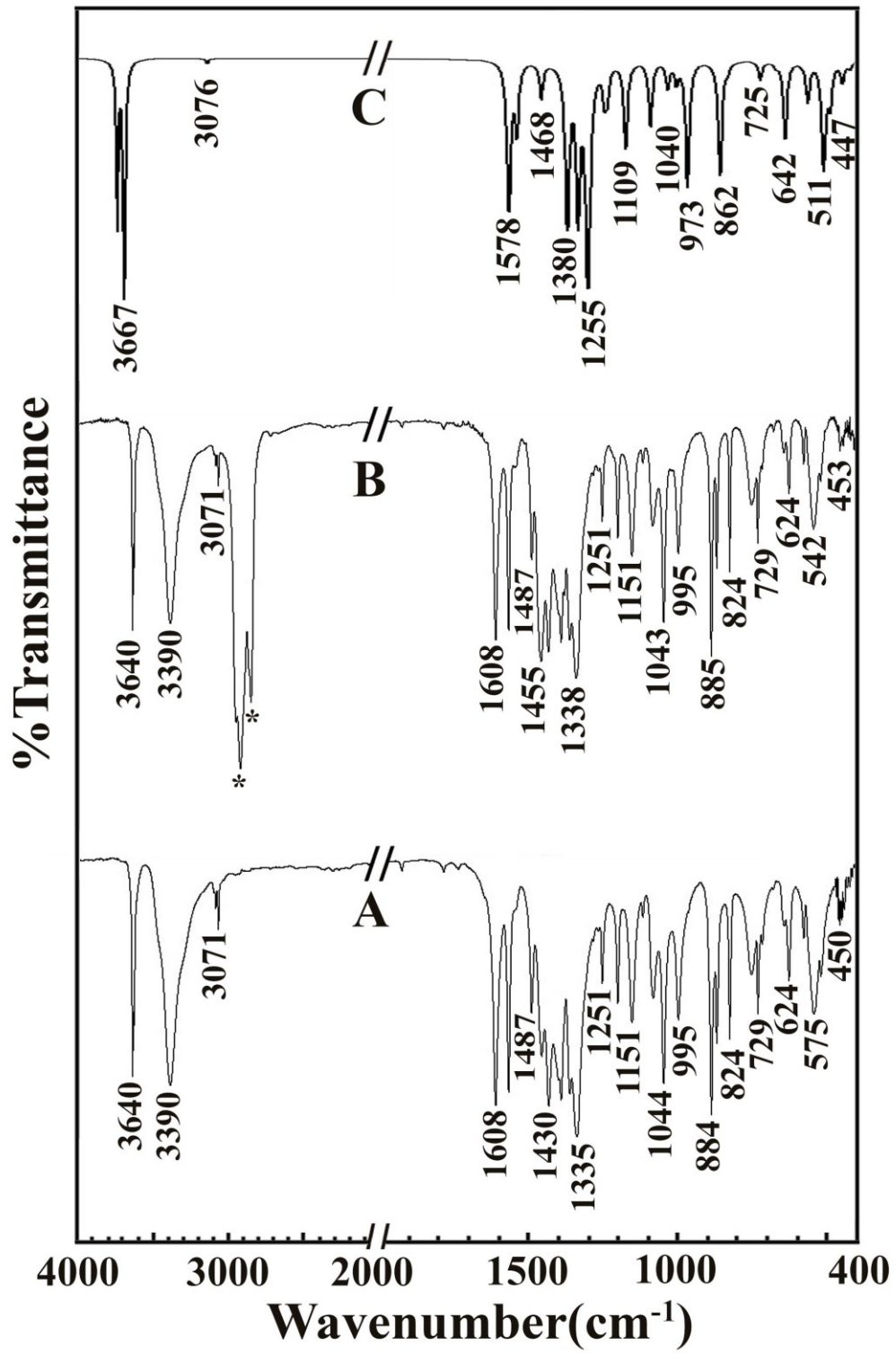


Fig. 2. IR spectrum in KBr disk of 2-Floro-4-chlorophenylboronic acid (A) from 400 to 4000 cm^{-1}; (B) Experimental IR spectrum in Nujol (C) scaled B3LYP/6-311++G(d,P) for 2-chloro-4-Florophenyl boronic acid (**CT**) conformer.

TABLE.2. Symmetry coordinates[a] for 2-Chloro-4-florophenylboronic acid, $C_6H_5FClBO_2$ (-d_0), $C_6H_3FClD_2BO_2$ (2OD)[b] and $C_6H_2FClD_3BO_2$ (3CD)[c] molecules.

ν_i[d]	Definition	Symmetry Coordinate
ν_1	OH/OD[b] Stretch	$S_1 = m_1 + m_2$
ν_2	OH/OD[b] Stretch	$S_2 = m_1 - m_2$
ν_3	CH/CD[c] Stretch	$S_3 = r_1 + r_2 + r_3$
ν_4	CH/CD[c] Stretch	$S_4 = 2r_1 - r_2 - r_3$
ν_5	CH/CD[c] Stretch	$S_5 = r_2 - r_3$
ν_6	CC Ring Stretch	$S_6 = q_1 + q_3 + q_5 - q_2 - q_4 - q_6$
ν_7	CC Ring Stretch	$S_7 = 2q_1 - q_3 - q_5 + 2q_2 - q_4 - q_6$
ν_8	CH/CD[c] In plan deformation	$S_8 = \alpha_1 - \alpha_2$
ν_9	CC Ring Stretch	$S_9 = q_3 - q_5 + q_4 - q_6$
ν_{10}	B−O Stretch	$S_{10} = a_1 + a_2$
ν_{11}	B−O Stretch	$S_{11} = a_1 - a_2$
ν_{12}	CC Ring Stretch	$S_{12} = 2q_1 - q_3 - q_5 - 2q_2 + q_4 + q_6$
ν_{13}	CH/CD[c] In plan deformation	$S_{13} = \alpha_3 - \alpha_4$
ν_{14}	C−F Stretch	$S_{14} = R$
ν_{15}	CH/CD[c] In plan deformation	$S_{15} = \alpha_5 - \alpha_6$
ν_{16}	C−B Stretch	$S_{16} = T$
ν_{17}	CC Ring Stretch	$S_{17} = q_3 - q_5 - q_4 + q_6$
ν_{18}	OH/OD[b] In plan deformation	$S_{18} = \lambda_1 - \lambda_2$
ν_{19}	OH/OD[b] In plan deformation	$S_{19} = \lambda_1 + \lambda_2$
ν_{20}	CH/CD[c] wag	$S_{20} = \gamma_1$
ν_{21}	Ring breath	$S_{21} = q_1 + q_3 + q_5 + q_2 + q_4 + q_6$
ν_{22}	CH/CD[c] wag	$S_{22} = \gamma_2$
ν_{23}	CH/CD[c] wag	$S_{23} = \gamma_3$
ν_{24}	CB wag	$S_{24} = \gamma_6$
ν_{25}	CCC Ring bending	$S_{25} = \theta_1 + \theta_3 + \theta_5 - \theta_2 - \theta_4 - \theta_6$
ν_{26}	Ring puckering	$S_{26} = \tau_1 - \tau_2 + \tau_3 - \tau_4 + \tau_5 - \tau_6$
ν_{27}	C−Cl Stretch	$S_{27} = E$
ν_{28}	OH/OD[b] torsion	$S_{28} = \eta_1$
ν_{29}	CF wag	$S_{29} = \gamma_5$
ν_{30}	CCC Ring bending	$S_{30} = \theta_2 - \theta_3 + \theta_5 - \theta_6$
ν_{31}	OH/OD[b] torsion	$S_{31} = \eta_2$
ν_{32}	C−F In plan deformation	$S_{32} = \beta_1 - \beta_2$
ν_{33}	Ring puckering	$S_{33} = \tau_1 - \tau_2 + \tau_4 - \tau_5$
ν_{34}	$B(OH)_2$ Scissor	$S_{34} = 2\Phi - \rho_1 - \rho_2$
ν_{35}	BO_2 Rock	$S_{35} = \rho_1 - \rho_2$
ν_{36}	CCC Ring bending	$S_{36} = 2\theta_1 - \theta_2 - \theta_3 + 2\theta_4 - \theta_5 - \theta_6$
ν_{37}	C−Cl In plan deformation	$S_{37} = \delta_1 - \delta_2$
ν_{38}	Ring twist	$S_{38} = \eta_3$
ν_{39}	CCl wag	$S_{39} = \gamma_4$

TABLE.2. Continued.

ν_i[d]	Definition	Symmetry Coordinate
ν_{40}	$CCB(OH)_2$ bending	$S_{40} = \varepsilon_1 - \varepsilon_2$
ν_{41}	Ring puckering	$S_{41} = 2\tau_3 - \tau_1 - \tau_2 + 2\tau_6 - \tau_4 - \tau_5$
ν_{42}	CCBO torsion	$S_{42} = \eta_4$

[a]Symmetry coordinates are not normalized.

[b]2-4-CFPB -d_2, $C_6H_3FClD_2BO_2$ deutrated two OH group.

[c]2-4-CFPB -d_3, $C_6H_2FClD_3BO_2$ deutrated three CH group.

[d]ν_{20},ν_{22}-ν_{24},ν_{26},ν_{28},ν_{29},ν_{31},ν_{33},ν_{38},ν_{39},ν_{41},ν_{42} belongs to A″ species and other symmetries belongs to A′species.

Overestimated due to systematic errors, including the neglect of electron correlation and basis set limitations [42]. Therefore, the wavenumbers calculated at the B3LYP/6-311++G(d,p) level were scaled by factors of 0.93 for stretches, 0.945 for in-plane deformations, and 0.978 for out-of-plane bending modes (wagging and torsions) to improve agreement with experimental values [43]. Furthermore, frequency calculations were performed for two isotopes of CFPB: C_2FPB-d_2 (O-D deuterated) and CFPB-d_3 (C-D deuterated). This helped to unequivocally distinguish between OH and CH bending modes and other fundamentals appearing in similar spectral regions. The final scaled harmonic vibrational frequencies, infrared intensities, Raman activities, and PEDs for all normal modes are presented in **Table 4**.

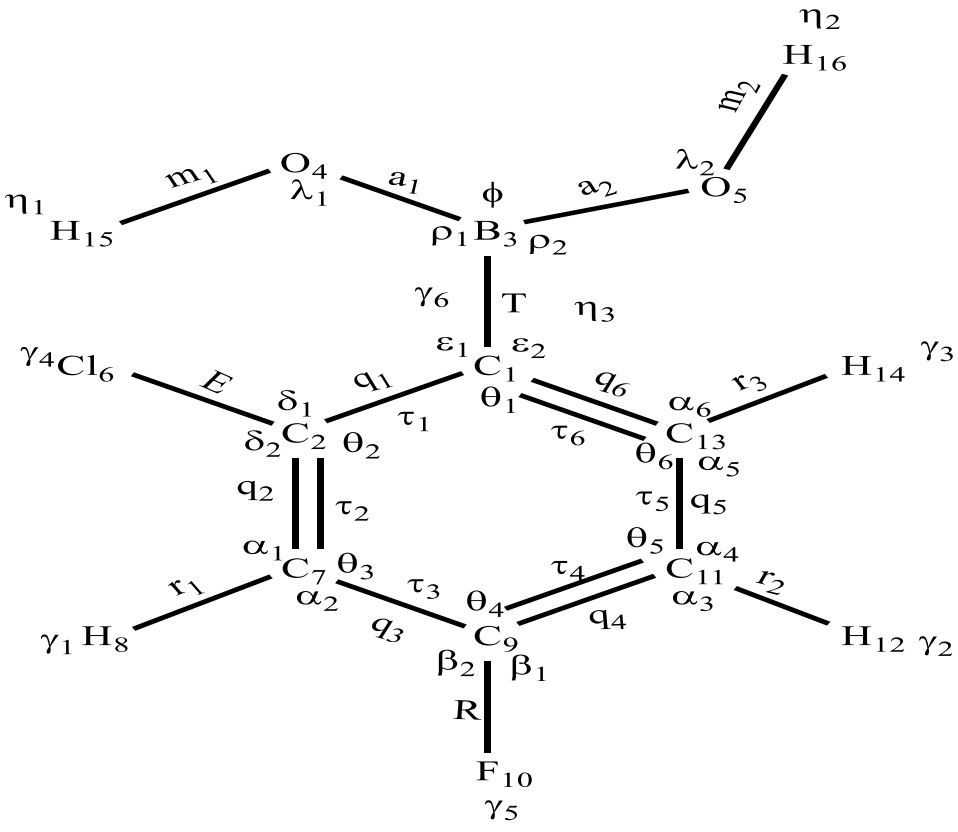


Fig. 3 Internal coordinates definition of 2-Chloro-4-fluorophenyl boronic acid(CFPB) **CT** coformer.

TABLE. 3. B3LYP/6-311++G(d,p) unscaled force constants (mdyne/Å) for 2-Chloro-4-florophenylboronic acid (conformer CT) molecule

Atom #	Vib. modes	Symbol[a]	Scaling factor[b]	Diagonal force constant[c]
C_1—C_2	Stretch	q_1	0.930	5.096
C_2—C_7	Stretch	q_2	0.930	5.192
C_7—C_9	Stretch	q_3	0.930	5.325
C_9—C_{11}	Stretch	q_4	0.930	5.320
C_{11}—C_{13}	Stretch	q_5	0.930	5.292
C_{13}—C_1	Stretch	q_6	0.930	4.801
C_1—B_3	Stretch	T	0.930	3.988
C_2—F_6	Stretch	R	0.930	6.389
C_9—Cl_{10}	Stretch	E	0.930	3.154
B_3—O_4	Stretch	a_1	0.930	6.034
B_3—O_5	Stretch	a_2	0.930	6.513
O_4H_{15}	Stretch	m_1	0.930	8.092
O_5H_{16}	Stretch	m_2	0.930	8.309
C_7H_8	Stretch	r_1	0.930	5.670
C_9H_{10}	Stretch	r_2	0.930	5.628
$C_{13}H_{14}$	Stretch	r_3	0.930	5.590
$B_3C_1C_2$	Bending	ε_1	0.945	1.030
$B_3C_1C_{13}$	Bending	ε_2	0.945	0.807
$C_1C_2F_6$	Bending	β_1	0.945	0.942
$C_7C_2F_6$	Bending	β_2	0.945	0.856
$C_7C_9Cl_{10}$	Bending	δ_1	0.945	0.663
$C_{11}C_9Cl_{10}$	Bending	δ_2	0.945	0.659
$C_2C_7H_8$	Bending	α_1	0.945	0.433
$C_9C_7H_8$	Bending	α_2	0.945	0.420
$C_9C_{11}H_{12}$	Bending	α_3	0.945	0.420
$C_{13}C_{11}H_{12}$	Bending	α_4	0.945	0.427
$C_{11}C_{13}H_{14}$	Bending	α_5	0.945	0.455
$C_1C_{13}H_{14}$	Bending	α_6	0.945	0.471
$C_1B_3O_4$	Bending	ρ_1	0.945	0.796
$C_1B_3O_5$	Bending	ρ_2	0.945	0.622
$O_4B_3O_5$	Bending	Φ	0.945	0.679
$H_{15}O_4B_3$	Bending	λ_1	0.945	0.626
$H_{16}O_5B_3$	Bending	λ_2	0.945	0.508
$C_{13}C_1C_2$	Bending	θ_1	0.945	0.787
$C_1C_2C_7$	Bending	θ_2	0.945	0.742
$C_2C_7C_9$	Bending	θ_3	0.945	0.708
$C_7C_9C_{11}$	Bending	θ_4	0.945	0.716
$C_9C_{11}C_{13}$	Bending	θ_5	0.945	0.706
$C_{11}C_{13}C_1$	Bending	θ_6	0.945	0.717
$C_2C_7H_8C_9$	Wag	γ_1	0.978	0.233
$C_9C_{11}H_{12}C_{13}$	Wag	γ_2	0.978	0.190
$C_{11}C_{13}H_{14}C_1$	Wag	γ_3	0.978	0.302
$C_1C_2F_6C_7$	Wag	γ_4	0.978	0.288
$C_7C_9Cl_{10}C_{11}$	Wag	γ_5	0.978	0.355
$C_2C_1B_3C_{13}$	Wag	γ_6	0.978	0.265
$C_2C_1B_3O_4$	Wag	η_3	0.978	0.705
$C_1B_3O_4H_{15}$	Torsion	η_1	0.978	0.139
$C_1B_3O_5H_{16}$	Torsion	η_2	0.978	0.120
$C_{13}C_1B_3O_5$	Torsion	η_4	0.978	0.424
$B_3C_1C_2C_7$	Puckering	τ_1	0.978	0.070
$C_1C_2C_7C_9$	Puckering	τ_2	0.978	0.165
$C_2C_7C_9C_{11}$	Puckering	τ_3	0.978	0.099
$C_7C_9C_{11}C_{13}$	Puckering	τ_4	0.978	0.077
$C_9C_{11}C_{13}C_1$	Puckering	τ_5	0.978	0.080
$C_{11}C_{13}C_1C_2$	Puckering	τ_6	0.978	0.104

[a]See **Fig. 2** for atom numbering and internal coordinates definitions.
[b]Implemented scaling factors to reproduce scaled frequencies in **Table 4**.
[c]Diagonal force constant at B3LYP/6-311++G(d,P) level.

3. Results and Discussion

3.1. Structural Parameters and Force Constants

As the crystal structure of CFPB is not available, the optimized structural parameters (SPs) were compared with experimental data for phenylboronic acid [16], 3-fluorophenylboronic acid [38], and 2,4-difluorophenylboronic acid [18]. The carbon-carbon bond distances show good agreement, typically within ±0.026 Å, and most bond angles align within ±0.1-7.2°. A notable exception is the ∠($B_3O_5H_{16}$) angle in 3-fluorophenylboronic acid [38], which deviates by about 13°. The calculated B–O bond distance of 1.366 Å is very close to the observed value of 1.359 Å for pentafluorophenylboronic acid [44], differing by only 0.007 Å. The calculated B–C bond distance of 1.579 Å also agrees well with X-ray data [16,38,18]. Substituting a C–H bond in benzene derivatives with a C–X (X = F, Cl, Br...) bond leads to a predictable increase in bond length [45]. For similar boronic acids [46,23,47], the observed C–Cl bond length ranges from 1.73 to 1.75 Å, which is consistent with our calculated value of 1.777 Å. Excellent correlations (R^2 values of 0.992, 0.985, and 0.984) were found between the experimental bond lengths [18,38,16] and those predicted by B3LYP/6-311++G(d,p). The CCC bond angles in the benzene ring range from 115.1° to 124.8° in our study, compared to 117.2°–121.8° in phenylboronic acid [16], 117.6°–123.9° in 3-fluorophenylboronic acid [38], and 114.6°–125.1° in 2,4-difluorophenylboronic acid [18]. The R^2 values for bond angles were 0.812 [18], 0.702 [38], and 0.683 [16]. Discrepancies in bond angles between experimental and theoretical values [16,18] are expected, as our calculations model an isolated molecule more representative of the gas phase, whereas X-ray data reflect the crystalline solid state. Overall, the predicted SPs show good agreement with X-ray data, particularly for bond distances. The calculated intramolecular hydrogen bond (HB) distances, O...H, range from 2.453 to 2.460 Å. These are shorter than the sum of the van der Waals radii for oxygen and hydrogen (2.72 Å) by 0.260–0.267 Å [48,49], indicating significant interaction. Similarly, the calculated Cl….H distances range from 2.194 to 2.200 Å, which are considerably shorter than the sum of the van der Waals radii for fluorine and hydrogen (3.0 Å) by 0.800–0.806 Å [50]. This suggests strong intramolecular HB interactions for O_5...H_{14} and Cl_6....H_{15}, in addition to the expected intermolecular HBs in the solid phase **(see Table 1)**.

3.2. Vibrational Assignments

The vibrational frequencies calculated using DFT methods show improved agreement with experimental values **(Table 4)**, suggesting that these methods partially account for anharmonic effects. Therefore, the vibrational assignments proposed here are primarily based on the B3LYP/6-311++G(d,p) frequencies compared to the observed wavenumbers [39]. The differences between the IR spectra obtained in KBr disk and Nujol mull were negligible (±2 cm^{-1}).

3.2.1. OH and CH Fundamental Vibrations

The assignments for the OH/OD and CH/CD stretching modes in C_2FPB **(Table 4)** are consistent with observed bands in the 3600–3000 cm^{-1} region. The O–H stretches were observed at 3640(s) and 3390(s, br), matching the calculated values at 3716 and 3667 cm^{-1}, respectively. These values align well with those reported for other boronic acid derivatives [1,16,21,23,24,26,51]. The O–H in-plane bending vibrations (δ_{ip}; ν_{17} and ν_{19}) were computed at 1040 and 973 cm^{-1}, corresponding well to the observed bands at 1044(s) and 884(s) cm^{-1}. Two OH out-of-plane bending modes are expected. The first, observed at 590 cm^{-1}, matches the calculated frequency at 585 cm^{-1} (ν_{28}). The second (δ_{oop}O–H), calculated at 511 cm^{-1} (ν_{31}), appears to be obscured in the low-wavenumber region below 541 cm^{-1}. These findings are consistent with both experimental data and literature reports [16,21,23,24,26,51].

The aromatic C–H stretching vibrations, typically observed between 3100 and 3000 cm^{-1}, are largely independent of the nature of the substituents [52-55]. Accordingly, the observed IR bands at 3095, 3085, and 3071 cm^{-1} are assigned to the C–H stretches (ν_3–ν_5), matching the calculated values at 3102, 3093, and 3076 cm^{-1}. Aromatic C–H in-plane deformation modes (δ_{ip}) for benzene derivatives generally fall in the 1300–1000 cm^{-1} range [56,57], while the out-of-plane deformations (δ_{oop}) occur between 1000 and 600 cm^{-1} [58]. The frequencies of these deformations are influenced more by the substituent's position than its identity [57,59]. In this study, the δ_{ip}CH modes (ν_8, ν_{13}, ν_{15}) were calculated at 1468, 1245, and 1109 cm^{-1}, aligning with the observed bands at 1487, 1198, and 1100 cm^{-1}. In agreement with Ref. [60], the observed IR bands at 866 and 824 cm^{-1} were assigned to δ_{oop} CH modes, corresponding to the predicted frequencies at 862 (ν_{22}) and 836 (ν_{23}) cm^{-1}. Notably, the δ_{ip} OH (ν_{19}) and a δ_{oop}CH (ν_{20}) mode, both calculated at 973 cm^{-1}, are likely overlapped and both contribute to the very strong IR band observed at 884 cm^{-1}.

TABLE.4. Observed and calculated frequencies (cm^{-1}) for 2-Chloro-4-florophenylboronic acid (CFPB) Structure CT.

Species	ν_i*	Assignment[a]	B3LYP/6-311++G(d,p)						
			Unscaled	Fixed[b] scaled	(X–D)[c]	IR Int[d].	Raman Act[e].	IR KBr[g]	PED[f]
	ν_1	υ_s OH / OD	3853	3716	2808	107.4	153.2	3640s	$51S_1\ 49S_2$
	ν_2	υ_s OH / OD	3803	3667	2790	206.7	50.3	3390s,br	$51S_2\ 49S_1$
	ν_3	υ_{as} CH / CD	3217	3102	2368	1.2	88.8	3095sh	$65S_3\ 35S_4$
	ν_4	υ_s CH / CD	3207	3093	2375	1.8	160.9	3085sh	$57S_4\ 29S_3\ 14S_5$
	ν_5	υ_{as} CH / CD	3189	3076	2340	0.22	47.1	3071wm	$86S_5\ 10S_4$
	ν_6	υ_s CC Ring	1633	1578		191.1	34.6	1608s	$34S_6\ 16S_7\ 16S_{16}\ 10S_{27}$
	ν_7	υ_s CC Ring	1606	1552		71.5	5.4	1564s	$50S_7\ 18S_6\ 10S_{29}$
	ν_8	δ_{ip} CH/ CD	1515	1468	914	35.1	2.8	1487m	$12S_8\ 22S_{13}\ 14S_6\ 13S_9\ 12S_{16}$
	ν_9	υ_s CC Ring	1426	1380		220.7	2.5	1430s	$14S_9\ 35S_{10}\ 10S_6 10S_{15}\ 10S_{16}$
A′	ν_{10}	υ_s B−O Stretch	1389	1344		209.2	5.9	1388s	$33S_{10}\ 12S_{12}\ 10S_9\ 10S_{14}\ 10S_{15}$
	ν_{11}	υ_s B−O Stretch	1355	1310		400.6	21.1	1335vs	$24S_{11}\ 20S_{16}\ 17S_{19}\ 10S_{10}\ 10S_{15}$
	ν_{12}	υ_s CC Ring	1296	1255		35.1	6.7	1251m	$50S_{12}\ 17S_{13}\ 10S_8$
	ν_{13}	δ_{ip} CH/ CD	1288	1245	850	31.0	3.8	1198m	$23S_{13}\ 30S_{12}\ 10S_7\ 10S_9\ 10S_{14}$
	ν_{14}	υ_s C−F Stretch	1222	1182		92.3	11.7	1151s	$35S_{14}\ 22S_8\ 20S_{20}\ 10S_{22}$
	ν_{15}	δ_{ip} CH/ CD	1143	1109	820	2.6	3.0	1100w	$41S_{15}\ 15S_{18}\ 13S_9\ 12S_{13}$
	ν_{16}	υ_s C−B Stretch	1133	1098		65.9	13.8	1079m	$38S_{16}\ 20S_{19}\ 18S_{20}\ 10S_9 10S_{22}$
	ν_{17}	δ_{ip} OH/ OD	1072	1040		24.9	2.0	1044s	$47S_{17}\ 10S_{18}\ 10S_{19}$
	ν_{18}	υ_s CC Ring	1041	1010	841	18.4	5.6	995s	$45S_{18}\ 22S_{17}\ 21S_{22}$
	ν_{19}	δ_{ip} OH/ OD	1004	973	800	150.8	1.7	(884vs)	$36S_{19}\ 38S_{11} 18S_{17}$
A″	ν_{20}	γ_{wag} CH / CD	983	973	810	0.22	0.04	(884vs)	$55S_{20}\ 18S_{23}\ 11S_{27}\ 10S_{40}$
A′	ν_{21}	Ring breath	892	863		93.8	13.8	(866s)	$22S_{21}\ 22S_{14}\ 20S_{25} 14S_{30}$
	ν_{22}	γ_{wag} CH / CD	872	862	757	37.7	0.13	(866s)	$65S_{22}\ 10S_{23}\ 10S_{27}$
A″	ν_{23}	γ_{wag} CH / CD	843	836	648	7.6	0.05	824m	$48S_{23}\ 26S_{20}\ 12S_{22}$
	ν_{24}	γ_{wag} CB	735	725		18.2	0.45	(729m)	$66S_{24}\ 11S_{29} 10S_{27}$
	ν_{25}	υ_s C−Cl Stretch	694	672		4.1	6.8	(729m)	$33S_{25}\ 55S_{34}$
A′	ν_{26}	δ_{ip} CCC Ring	663	642		17.5	5.8	638sh	$14S_{26}$ $27S_{16} 13S_{30} 11S_{11} 10S_{14} 10S_{32}$
A″	ν_{27}	δ Ring puckering	650	641		60.8	0.20	624m	$25S_{27}\ 45S_{24}\ 21S_{33}$
A″	ν_{28}	τ OH/ OD	592	585	442	1.4	0.24	590w	$63S_{28} 16S_{33} 15S_{37}$
	ν_{29}	γ_{wag} C−F	569	564		41.2	0.21	575m	$21S_{29}\ 29S_{40}\ 24S_{28}\ 19S_{31}$
A′	ν_{30}	δ_{ip} CCC Ring	517	502		11.6	1.5	541br,m	$23S_{30}\ 17S_{32}\ 16S_{34}\ 13S_{38} 10S_{39}$
A″	ν_{31}	τ OH/ OD	518	511	380	118.2	1.9	—	$72S_{31}\ 10S_{28}\ 10S_{29}$
A′	ν_{32}	δ_{ip} C−F	504	489		38.6	3.0	(450w)	$18S_{32}\ 34S_{36}\ 15S_{30}\ 10S_{38}\ 10S_{39}$
A″	ν_{33}	δ Ring puckering	452	447		18.3	0.54	(450w)	$26S_{33}\ 16S_{41}\ 13S_{40} 10S_{23} 10S_{29}$
	ν_{34}	δ_{ip} CCC Ring	435	422		6.0	8.3	(450w)	$28S_{34}\ 28S_{25}\ 18S_{32}\ 10S_{21}$
A′	ν_{35}	δ_{Rock} BO_2	344	334		5.1	2.2	—	$35S_{35}\ 22S_{32} 18S_{25}$
	ν_{36}	$\delta_{Scissor}$ $B(OH)_2$	322	312		3.9	3.3	—	$23S_{36}\ 29S_{30}\ 23S_{16}\ 10S_{35}$
A″	ν_{37}	Ring Twist	284	281		1.8	2.0	—	$59S_{37}\ 22S_{27}$

	ν_{38}	δ_{ip} C–Cl	247	240	0.78	1.3	—	$70S_{38}\ 10S_{32}$
A′	ν_{39}	$CCB(OH)_2$ bending	187	182	3.7	0.33	—	$69S_{39}\ 22S_{35}$
	ν_{40}	γ_{wag} CCl	180	176	0.01	0.77	—	$25S_{40}\ 20S_{41}\ 16S_{22}11S_{27}10S_{33}$
	ν_{41}	δ Ring puckering	99	99	0.93	1.0	—	$35S_{41}\ 33S_{33}\ 15S_{42}$
	ν_{42}	τ CCBO	29	28	1.0	0.05	—	$85S_{42}\ 10S_{33}$

a Notations for fundamentals: m, stretch; d, bending; c, wagging; R, ring and s, torsion. These fundamentals could be pure in minor cases; however they are coupled with other normal modes as given in PEDs.
b Scaling factors 0.93 for all stretches. Moreover 0.945 used for bends and 0.978 for wags and torsions.
c The calculated unscaled frequencies for d_1-4-2-CFPB (X-D = C-D or O-D) isotopmers.
d Calculated infrared intensities in km/mol (IUPAC, Glossary of terms used in Photochemistry, 3rd Edition, July 2004).
e Calculated Raman activities in Å4/amu.
f Contributions less than 10% are omitted.
g Bands between brackets are used for two or three normal modes of vibration.

3.2.2. $B(OH)_2$ Fundamental Vibrations

The B–O stretching frequency typically gives rise to a strong band in the 1300–1400 cm^{-1} region in FT-IR spectra [1,21,23,24,26,51]. Vargas et al. assigned the ν(B–O) stretch in trinuclear boron complexes around 1370 cm^{-1} [61]. In our study, the B–O stretching modes are calculated at 1344 (ν_{10}) and 1310 (ν_{11}) cm^{-1}, fitting the observed IR bands at 1388 and 1335 cm^{-1}, respectively. Fundamentals below 400 cm^{-1} namely the $B(OH)_2$ scissoring mode (ν_{35}), the BO_2 rocking (ν_{35}), CCB bending (ν_{40}), and torsion (ν_{42}) modes fall outside our experimental range and could not be observed.

3.2.3. C–X (X = B, F, Cl) Fundamental Vibrations

Three C–X (X = B, F, Cl) stretches are expected in the solid-state IR spectrum of C_2FPB. The C–F and C–Cl stretching frequencies produce strong and medium IR bands, respectively. Their predicted infrared intensities (92.3 and 4.1 km/mol) support their assignment to the observed bands at 1151 cm^{-1} and 729 cm^{-1}, consistent with literature [23,24,26]. The C–B stretch (ν_{16}) is observed at 1098 cm^{-1} and calculated at 1079 cm^{-1}, agreeing well with a reported value of 1085 cm^{-1} [62], though this mode is sometimes overlooked [1]. Furthermore, the observed IR bands at 729 and 575 cm^{-1} are assigned to the C–B (ν_{24}) and C–F (ν_{29}) wagging modes, respectively. The C–Cl in-plane (ν_{38}) and out-of-plane (ν_{40}) bends were predicted at 240 and 176 cm^{-1} but could not be observed experimentally, as mentioned.

3.2.4. Ring Fundamental Vibrations

Ring stretching vibrations were predicted in the 1600–865 cm^{-1} range, consistent with similar molecular systems [1,16,21,23,24,26,58,63]. The computed wavenumbers show slight deviations from the observed values but are supported by their predicted IR intensities. The observed bands at 1609 (ν_6), 1564 (ν_7), and 1430 (ν_9) cm^{-1} correspond to calculated intensities of 191.1, 71.5, and 220.7 km/mol, respectively. The medium and strong IR bands at 1251 (ν_{12}) and 995 (ν_{18}) cm^{-1} match the calculated values at 1255 and 1010 cm^{-1}. The ring breathing mode (ν_{21}) is assigned to the strong band at 866 cm^{-1}, consistent with its high predicted IR intensity of 93.8 km/mol. The ring deformation modes (ν_{26} and ν_{30}), calculated at 642 and 502 cm^{-1}, fit the observed bands at 638 and 541 cm^{-1}, in agreement with experimental values [64,65]. Other fundamentals (ν_{37}, ν_{41}) lie below 400 cm^{-1} and were not observed.

3.3. OH Barriers to Internal Rotation

The 3D potential energy surface for the rotation of both the hydroxyl groups in the CT conformer was explored. The O_5H_{16} (*trans*) and O_4H_{15} (*cis*) group was rotated in 10° increments around the C–B bond together at same time to determine any other minimum structure **(Fig. 4)**. Starting from the TC (E = -967.278089 Hartree), the energy increased to a maximum at a dihedral angle $\tau(H_{15}O_4B_3C_1)$ of -100° and $\tau(H_{16}O_4B_3C_1)$ of 80° (E = -967.249231 Hartree), corresponding to a nearly perpendicular OH orientation relative to the benzene ring. Further rotation led to a decrease in energy toward the CT conformer minimum. The barrier between this maximum and the CT isomer is 22.2 kcal/mol (7749 cm^{-1}). The barrier from TT to CT was found to be 6.7 kcal/mol (2356 cm^{-1}).

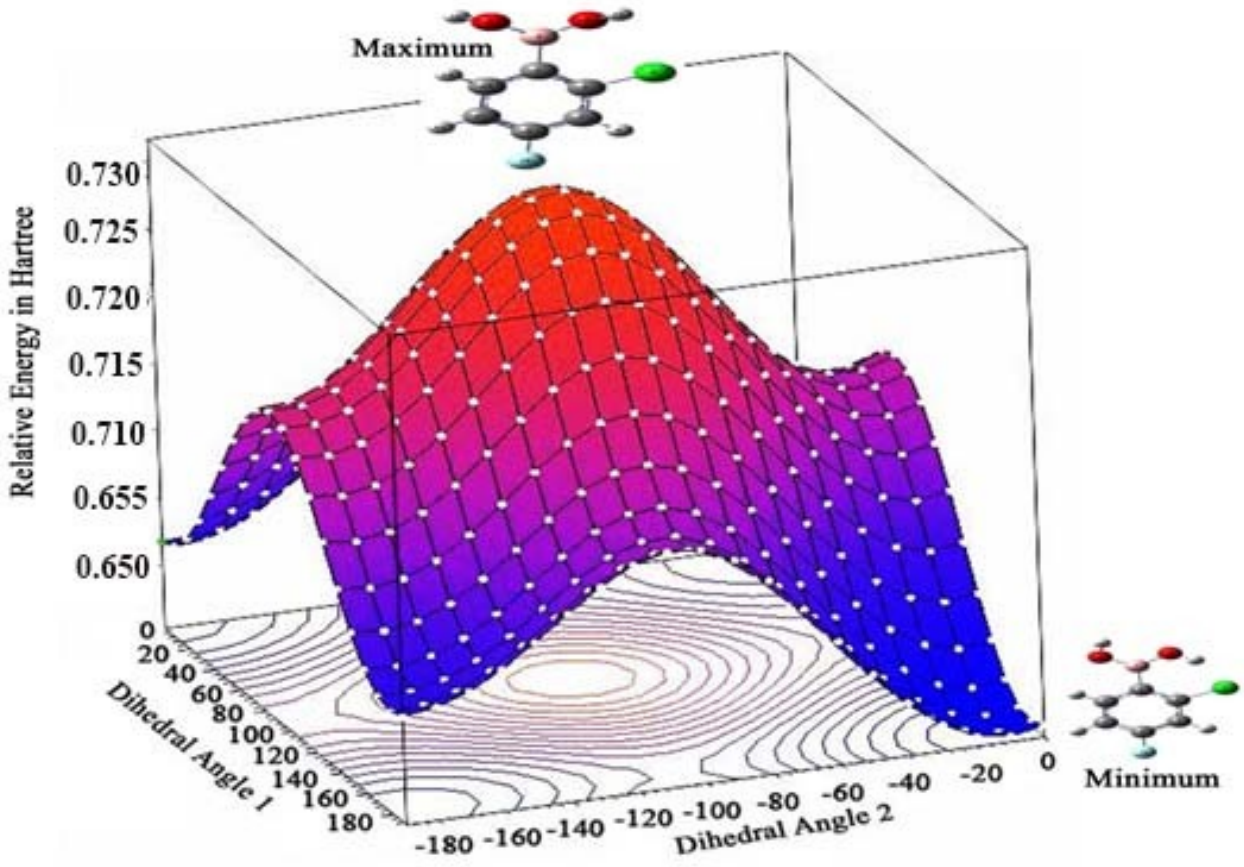


Fig. 4. 3D Barriers to internal rotations of two OH groups of 2-Chloro-4-fluorophenyl boronic acid as obtained from B3LYP /6-311++G(d,p) potential surface scan.

The barrier between CC to CT barrier is 4.9 kcal/mol (1722 cm^{-1}). These values are consistent with V_2 barriers reported for 2-aminophenol and p-fluorophenol (1213 and 1007 cm^{-1}, respectively) [63,66,67]. These significant rotational barriers, along with the calculated imaginary frequencies for other conformers, firmly justify the exclusion of high-energy isomers and confirm CT as the most stable structure.

4. Conclusion

B3LYP/6-311++G(d,p) computations establish that the **CT** conformer of **(2-chloro-4-fluorophenyl)boronic acid** is the most stable structure in the solid phase. In this conformation, one OH group is *cis* to the phenyl C_1 and Cl atoms, while the other is *trans* to the phenyl C_1 atom. Supported by frequency calculations, normal coordinate analysis, and experimental IR spectroscopy, comprehensive and accurate vibrational assignments have been proposed for all observed fundamental modes.

Funding

The authors declare that this research received no external funding.

Data Availability Statement

Not applicable.

Conflicts of Interest

The authors declare no conflict of interest.

References

[1] Mariana Pereira Silva, Lucília Saraiva, Madalena Pinto and Maria Emília Sousa, Boronic Acids and Their Derivatives in Medicinal Chemistry: Synthesis and Biological Applications. *Molecules* **2020**, *25*(18), 4323; https://doi.org/10.3390/molecules25184323

[2] Deniz A. Anakök, Andrea Angeli, Ilaria D'Agostino, Gioele Renzi, Maria Luisa Massardi, Camilla Tavani, Servet Çete, Simone Carradori, Roberto Ronca, Clemente Capasso, Fabrizio Carta, Claudiu T. Supuran, A Journey Around Boronic Acids: Sulfonyl Hydrazone-Containing Derivatives as Carbonic Anhydrase Inhibitors. *Chemical Biology & Drug Design* **09 April 2025,** 105(4), e70108; *https://doi.org/10.1111/cbdd.70108*

[3] Hall, D. G. *Boronic Acids: Preparation and Applications in Organic Synthesis and Medicine*; Wiley-VCH: Weinheim, 2005.

[4] Suzuki, A. Cross-Coupling Reactions Of Organoboranes: An Easy Way To Create C–C Bonds. *Angew. Chem. Int. Ed.* **2011**, *50* (30), 6722–6737.

[5] Yang, W.; Gao, X.; Wang, B. Boronic Acid Compounds as Potential Pharmaceutical Agents. *Med. Res. Rev.* **2003**, *23* (3), 346–368.

[6] Bull, S. D.; Davidson, M. G.; Van den Elsen, J. M. H.; Fossey, J. S.; Jenkins, A. T. A.; Jiang, Y.-B.; Kubo, Y.; Marken, F.; Sakurai, K.; Zhao, J.; James, T. D. Boronic Acid-Based Sensor. *Acc. Chem. Res.* **2019**, *52* (10), 2879–2890.

[7] Wu, X.; Li, Z.; Chen, X.-X.; Fossey, J. S.; James, T. D.; Jiang, Y.-B. Selective Sensing of Saccharides Using Simple Boronic Acids and Their Aggregates. *Chem. Soc. Rev.* **2013**, *42* (20), 8032–8048.

[8] Rettig, S. J.; Trotter, J. Refinement of the Crystal Structure of Phenylboronic Acid. *Can. J. Chem.* **1977**, *55* (17), 3071–3075.

[9] Kurt, M. Theoretical and Experimental Study on the Molecular Structure and Vibration Spectra of 4-Chlorophenylboronic Acid. *J. Mol. Struct.* **2009**, *919* (1–3), 215–223.

[10] Karabacak, M.; Kose, E.; Atac, A.; Sas, E. B.; Asiri, A. M.; Kurt, M. Experimental (FT-IR, FT-Raman, UV and NMR) and Theoretical (EHMO and DFT) Analysis of 3-Bromophenylboronic Acid. *Spectrochim. Acta A* **2012**, *97*, 892–904.

[11] Rodríguez-Cuamatzi, P.; Vargas-Díaz, G.; Hopfl, H. 2,4-Difluorophenylboronic Acid. *Acta Crystallogr. E* **2005**, *61* (6), o44–o46.

[12] Frisch, M. J.; Trucks, G. W.; Schlegel, H. B.; Scuseria, G. E.; Robb, M. A.; Cheeseman, J. R.; Scalmani, G.; Barone, V.; Mennucci, B.; Petersson, G. A.; et al. *Gaussian 09, Revision D.01*; Gaussian, Inc.: Wallingford, CT, 2009.

[13] Becke, A. D. Density-Functional Exchange-Energy Approximation with Correct Asymptotic Behavior. *Phys. Rev. A* **1988**, *38* (6), 3098–3100.

[14] Lee, C.; Yang, W.; Parr, R. G. Development of the Colle-Salvetti Correlation-Energy Formula into a Functional of the Electron Density. *Phys. Rev. B* **1988**, *37* (2), 785–789.

[15] Vosko, S. H.; Wilk, L.; Nusair, M. Accurate Spin-Dependent Electron Liquid Correlation Energies for Local Spin Density Calculations: A Critical Analysis. *Can. J. Phys.* **1980**, *58* (8), 1200–1211.

[16] Wilson, E. B.; Decius, J. C.; Cross, P. C. *Molecular Vibrations: The Theory of Infrared and Raman Vibrational Spectra*; McGraw-Hill: New York, 1955.

[17] NIST Computational Chemistry Comparison and Benchmark Database, NIST Standard Reference Database Number 101, Release 22, May 2024.

[18] Sass, E.; Kose, E.; Kurt, M.; Karabacak, M. FT-IR, FT-Raman, Molecular Structure and Natural Bond Orbital Analysis of 2-Fluorophenylboronic Acid. *Spectrochim. Acta A* **2015**, *137*, 1315–1325.

[19] Yang, W.; He, H.; Drueckhammer, D. G. Computer-Guided Design in Molecular Recognition: Design and Synthesis of a Glucopyranose Receptor. *Angew. Chem. Int. Ed.* **2001**, *40* (9), 1714–1718.

[20] Larsen, R. D.; King, A. O.; Chen, C. Y.; Corley, E. G.; Foster, B. S.; Roberts, F. E.; Yang, C.; Lieberman, D. R.; Reamer, R. A. Efficient Synthesis of Losartan, A Nonpeptide Angiotensin II Receptor Antagonist. *J. Org. Chem.* **1994**, *59* (21), 6391–6394.

[21] Tjarks, W.; Anisuzzaman, A. K. M.; Liu, L.; Soloway, A. H.; Barth, R. F.; Perkins, D. J.; Adams, D. M. Synthesis and in Vivo Evaluation of Bis-Mercaptoundecahydro-Closo-Dodecaborate Derivatives. *J. Med. Chem.* **1992**, *35* (9), 1628–1633.

[22] Yamamoto, Y.; Asao, N. Selective Reactions Using Allylic Metals. *Chem. Rev.* **1993**, *93* (6), 2207–2293.

[23] Alam, F.; Soloway, A. H.; Barth, R. F.; Mafune, N.; Adams, D. M.; Knoth, W. H. Boron Neutron Capture Therapy: Linkage of a Boronated Macrocyclic Molecule to Monoclonal Antibodies. *J. Med. Chem.* **1989**, *32* (10), 2326–2330.

[24] O'Donovan, M. R.; Mee, C. D.; Fenner, S.; Teasdale, A.; Phillips, D. H. Boronic Acids-A Novel Class of Bacterial Mutagen. *Mutat. Res.* **2011**, *724* (1–2), 1–6.

[25] Cambre, J. N.; Sumerlin, B. S. Biomedical Applications of Boronic Acid Polymers. *Polymer* **2011**, *52* (21), 4631–4643.

[26] Westmark, P. R.; Smith, B. D. Boronic Acid Sensors for Saccharides. *J. Pharm. Sci.* **1996**, *85* (3), 266–269.

[27] Cyranski, M. K.; Jezierska, A.; Klimentowska, P.; Panek, J. J.; Sporzynski, A. On the Aromatic Character of the Benzene Ring in Substituted Benzenes. *J. Phys. Org. Chem.* **2008**, *21* (6), 472–482.

[28] Faniran, J. A.; Shurvell, H. F. Infrared Spectra of Phenylboronic Acid and Diphenyl Phenylboronate. *Can. J. Chem.* **1968**, *46* (12), 2089–2095.

[29] Kurt, M. FT-Raman and FT-IR Spectra and DFT Calculations of 4-Chlorophenylboronic Acid. *J. Raman Spectrosc.* **2009**, *40* (1), 67–75.

[30] Karabacak, M.; Cinar, M.; Kurt, M. Molecular Structure and Vibrational Spectra of 3,5-Dichlorophenylboronic Acid. *J. Mol. Struct.* **2008**, *885* (1–3), 28–35.

[31] Rai, A. K.; Kumar, S.; Rai, A. K. Vibrational Spectra of 2,6-Dimethoxyphenylboronic Acid. *Vib. Spectrosc.* **2007**, *42* (2), 397–403.

[32] Rettig, S. J.; Trotter, J. Crystal Structure of Phenylboronic Acid. *Can. J. Chem.* **1977**, *55* (17), 3071–3075.

[33] Cyranski, M. K.; Jezierska, A.; Klimentowska, P.; Panek, J. J.; Sporzynski, A. Structural and Energetic Analysis of Molecular Crystals of Phenylboronic Acid. *J. Phys. Org. Chem.* **2008**, *21* (6), 472–482.

[34] Rodríguez-Cuamatzi, P.; Vargas-Díaz, G.; Hopfl, H. Crystal Structure of 2,4-Difluorophenylboronic Acid. *Acta Crystallogr. E* **2005**, *61* (6), o44–o46.

[35] Frisch, M. J.; Trucks, G. W.; Schlegel, H. B.; Scuseria, G. E.; Robb, M. A.; Cheeseman, J. R.; Scalmani, G.; Barone, V.; Mennucci, B.; Petersson, G. A.; et al. *Gaussian 09, Revision D.01*; Gaussian, Inc.: Wallingford, CT, 2009.

[36] Becke, A. D. Density-Functional Thermochemistry. III. The Role of Exact Exchange. *J. Chem. Phys.* **1993**, *98* (7), 5648–5652.

[37] Lee, C.; Yang, W.; Parr, R. G. Development of the Colle-Salvetti Correlation-Energy Formula into a Functional of the Electron Density. *Phys. Rev. B* **1988**, *37* (2), 785–789.

[38] Vosko, S. H.; Wilk, L.; Nusair, M. Accurate Spin-Dependent Electron Liquid Correlation Energies for Local Spin Density Calculations: A Critical Analysis. *Can. J. Phys.* **1980**, *58* (8), 1200–1211.

[39] Pulay, P. Ab Initio Calculation of Force Constants and Equilibrium Geometries in Polyatomic Molecules. *Mol. Phys.* **1969**, *17* (2), 197–204.

[40] Schlegel, H. B. Optimization of Equilibrium Geometries and Transition Structures. *J. Comput. Chem.* **1982**, *3* (2), 214–218.

[41] Hehre, W. J.; Radom, L.; Schleyer, P. v. R.; Pople, J. A. *Ab Initio Molecular Orbital Theory*; Wiley: New York, 1986.

[42] Peng, C.; Ayala, P. Y.; Schlegel, H. B.; Frisch, M. J. Using Redundant Internal Coordinates to Optimize Equilibrium Geometries and Transition States. *J. Comput. Chem.* **1996**, *17* (1), 49–56.

[43] Wilson, E. B.; Decius, J. C.; Cross, P. C. *Molecular Vibrations: The Theory of Infrared and Raman Vibrational Spectra*; McGraw-Hill: New York, 1955.

[44] Schachtschneider, J. H. *Vibrational Analysis of Polyatomic Molecules*; Shell Development Co.: Houston, TX, 1964–1965.

[45] NIST Computational Chemistry Comparison and Benchmark Database. http://cccbdb.nist.gov/vibscale.asp (accessed May 2024).

[46] Wu, Y.; Dong, C.; Liu, S.; Zhu, H.; Wu, M. Y. Crystal Structure of 3-Fluorophenylboronic Acid. *Acta Cryst. E* **2006**, *62* (6), o4236–o4237.

[47] Horton, P. N.; Hursthouse, M. B.; Becket, M. A.; Hankey, M. A. Crystal Structure of Pentafluorophenylboronic Acid. *Acta Cryst. E* **2004**, *60* (12), o2204–o2205.

[48] Shimpl, M.; Seetha, N. L.; Pedireddi, V. R. Crystal Structures of 4-Chloro- and 4-Bromophenylboronic Acids. *Cryst. Growth Des.* **2007**, *7* (10), 1958–1963.

[49] David, J.; Hallam, H. E. Infrared Spectra of Boronic Acids and Their Anhydrides. *Spectrochim. Acta* **1965**, *21* (5), 841–848.

[50] Krueger, P. J. Vibrational Spectra of Boron Compounds. *Tetrahedron* **1970**, *26* (22), 4753–4766.

[51] Karabacak, M.; Kurt, M. FT-IR, FT-Raman and DFT Studies of 2,3-Difluorophenylboronic Acid. *J. Mol. Struct.* **2009**, *919* (1–3), 215–223.

[52] Socrates, G. *Infrared and Raman Characteristic Group Frequencies: Tables and Charts*, 3rd ed.; John Wiley & Sons: Chichester, 2001.

[53] Dwivedi, C. P.; Sharma, S. N. Vibrational Spectra of Substituted Benzenes. *Indian J. Pure Appl. Phys.* **1973**, *11* (6), 447–452.

[54] Varsanyi, G. *Assignments for Vibrational Spectra of Seven Hundred Benzene Derivatives*; Adam Hilger: London, 1974.

[55] Singh, N. P.; Yadav, R. A. Vibrational Spectra of Chloro- and Fluorobenzenes. *Indian J. Phys. B* **2001**, *75* (4), 347–352.

[56] Doddamani, S.; Ramoji, A.; Yenagi, J.; Tonannavar, J. Vibrational Spectra of Disubstituted Benzenes. *Spectrochim. Acta A* **2007**, *67* (1), 150–156.

[57] Jag, M. *Organic Spectroscopy - Principles and Applications*; Narosa Publishing House: New Delhi, 2001.

[58] Balachandran, V.; Parimala, K. Vibrational Spectroscopic Studies of 2,4-Dichlorophenylboronic Acid. *J. Mol. Struct.* **2012**, *1007*, 136–146.

[59] Kalsi, P. S. *Spectroscopy of Organic Compounds*, 6th ed.; New Age International: New Delhi, 2004.

[60] Jag, M. *Organic Spectroscopy: Principles and Applications*, 2nd ed.; Narosa Publishing House: New Delhi, 2010.

[61] Vargas, G.; Hernandez, I.; Hopfl, H.; Ochoa, M. E.; Castillo, D.; Farfan, N.; Santillan, R.; Gomez, E. Trinuclear Boron Complexes. *Inorg. Chem.* **2004**, *43* (3), 8490–8497.

[62] Romanos, J.; Beckner, M.; Stalla, D.; Tekcei, A.; Suppes, G.; Jalisatgi, S.; Lee, M. W.; Hawthorne, M. F.; Robertson, J. D.; Firlej, L.; et al. Infrared Spectroscopy of Boron Compounds. *Carbon* **2013**, *54*, 208–212.

[63] Soliman, U. A.; Hassan, A. M.; Mohamed, T. A. Vibrational Analysis of 2-Aminophenol. *Spectrochim. Acta A* **2007**, *68* (3), 688–696.

[64] Yamaguchi, Y.; Frisch, M.; Gaw, J.; Schaefer, H. F.; Binkley, J. S. Analytical Second Derivatives for Molecular Orbital Theory. *J. Chem. Phys.* **1986**, *84* (4), 2262–2268.

[65] Sathyanarayanan, D. *Vibrational Spectroscopy: Theory and Applications*; New Age International: New Delhi, 2004.

[66] Larsen, N. W.; Nicolaisen, F. M. Vibrational Spectra and Conformational Analysis of p-Fluorophenol. *J. Mol. Struct.* **1979**, *22* (1), 29–36.

[67] Martinez de la Hoz, J. M.; Balbuena, P. B. The DFT Route to Geometry Optimization and Vibrational Spectrum Calculation. In *Density Functional Theory*; IntechOpen: London, 2013; pp 277–301.